24th International Conference & Exhibition on Electricity Distribution (CIRED)

12-15 June 2017

Session 2: Power quality and electromagnetic compatibility

Control strategy for reactive power and harmonic compensation of three-phase grid-connected photovoltaic system

ISSN 2515-0855
doi: 10.1049/oap-cired.2017.1009
www.ietdl.org

Mehrdad Tarafdar Hagh ✉, *Mohammad Jadidbonab, Mahdi Jedari*

Faculty of Electrical and Computer, Engineering University of Tabriz, Iran
✉ *E-mail: tarafdar@tabrizu.ac.ir*

Abstract: This study investigates a grid-tied photovoltaic (PV) system with active power injection, reactive power compensation and harmonic current elimination capability. The equivalent electric model presented in the literature is used to implement the PV system. In non-linear loads, low-frequency synchronous reference frame (SRF) methods cannot eliminate second- and third-order harmonics which appear in the grid current. In this study, a mathematical analytical SRF approach is proposed to compensate reactive power and eliminate current harmonic of a non-linear load with active power injection. Simulation results are presented in order to verify the suggested control approach and the system feasibility.

1 Introduction

In recent years, investigations on alternative energy sources at national and global levels have been raised significantly. This is caused by increased electrical energy demand, besides concerns about conventional electrical energy sources reduction or extinction, mainly the fossil fuel and nuclear sources. Generally, the conventional electrical energy generation burns fossil fuel and mineral coal fuel, which emits pollutants into the environment. Thus, causes significant environmental impacts. The nuclear production systems have catastrophic risks, as large environmental impacts of hydroelectric power plants.

The alternative and renewable electrical sources can revolutionise conventional electrical energy production, which has minimum ecological and economic impacts. There are different types of alternative and renewable electrical energy sources such as hydropower, biomass, wind, sea and photovoltaic (PV).

Solar energy can be used as electrical energy by PV panels in the electrical energy conversion process [1]. The most beneficial natural energy source is the electrical energy produced by PV system [2].

The PV array employs the photoelectric effect to transform the light energy into electrical power [3], which is clean and has nearly no environmental impact. There is a little waste during the manufacturing process, which is removed in the process and makes this energy as desirable sources for future. Besides, there is a need for a sufficient energy conversion stage to inject energy produced by the PV into the power grid. In another word, there is a need for accommodation between the PV DC energy and the grid AC energy. Typically, two power converters, i.e. a DC/DC converter to boost the PV voltage and a DC/AC inverter to transform the DC voltage to AC are needed.

Besides, the most crucial issue of energy generation from renewable sources has been well discussed during past years, which is related to the electrical power systems power quality (PQ). Thus, utilisation of non-linear loads by industrial and commercial sectors besides domestic consumers increases PQ problems. These loads draw high contents harmonics from the power grid, which decreases electrical power systems PQ.

The interaction between harmonic currents and network line impedance causes voltage harmonic distortion that influences on the all consumers PQ connected to the same point of common coupling in the electrical system [4]. Moreover, it can cause extreme heating of transformers and electrical facilities, increase noise frequency and electric motors electromagnetic torque oscillations.

A solution to decrease these PQ problems is the utilisation of shunt active power filters (APFs) [5], which can eliminate or mitigate the effects caused by the circulation of harmonic currents introduced by non-linear loads [6].

In this paper, an integration of a three-phase grid-tied PV and an active filter abbreviated as (PV–AF) system with an analytical synchronous reference frame (SRF) control approach is studied. The system is connected to the power grid through a full-bridge converter to fulfil the following functions: maximum power point tracking (MPPT), injecting active power into the power grid, performing active filtering and reactive compensation, simultaneously.

2 Overall system power structure

The PV–AF system that is implemented in this paper is assumed that a PV array constituted of ten panels connected in series, adopting the Sun-Power SPR-305WHT PV model. Therefore, it can acquire 30 kW of total output power.

The system which is used to implement PV array is briefly outlined in the next section. Furthermore, in the latter sections the current reference generation algorithm and the hysteresis pulse width modulation (PWM) technique employed in the PV–AF system are explained.

Fig. 1 shows the control system of PV system.

2.1 DC voltage regulation

A method is used to regulate the DC-bus voltage of the PV–AF system. The DC-bus voltage is regulated according to the available power of the PV array, when the PV array produces enough electrical energy, because of the solar irradiation and temperature conditions are favourable, the DC-bus reference voltage is set to be equal to the PV array output voltage.

In this case, the active power drained from PV is provided to the load and its surplus is injected into the grid. As can be outstanding, the active energy of the load is shared between the grid and the PV–AF system, while the PV–AF system accomplishes steadily the shunt-APF function.

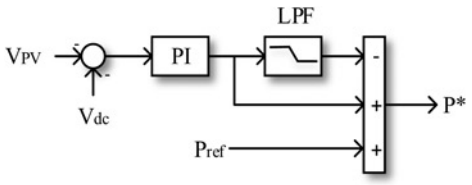

Fig. 1 *Control system of PV*

2.2 PV panel modelling

Fig. 2 shows the equivalent circuit of the PV panel with single diode model.

With neglecting R_p, the relation for determining the I–V behaviour of single diode model is expressed as

$$I = I_{\text{pv}} - I_0\left[\exp\left\{\frac{q(V + R_{\text{s}}I)}{KAT}\right\}\right] - 1 \tag{1}$$

where I_{pv} is the irradiance photocurrent current, I_0 is the diode reverse saturation current, q is the electron charge, K is the Boltzmann's constant, A is the diode ideality factor, T is the PV array operating temperature in kelvin, R_{s} is the series resistance, V is the PV array terminal voltage and I is the PV array terminal current.

Series and parallel connections of PV panels forms a PV cell. Suppose a PV panel with n_{s} number of series arrays and n_{p} number of parallel arrays. The mathematical relation (1) will modify to (2) as follows:

$$I = n_pI_{\text{pv}} - n_pI_0\left[\exp\left\{\frac{q(n_pv + n_{\text{s}}IR_{\text{s}})}{n_{\text{s}}n_pKAT}\right\} - 1\right] \tag{2}$$

Solar radiation and PV panel operating temperature contributes in photocurrent, which is concluded in (3) as follows:

$$I_{\text{pv}} = [I_{\text{sc}} + \alpha(T - T_{\text{r}})]G \tag{3}$$

where I_{sc}, α, T_{r} and G are short-circuit current, temperature coefficient of PV array short circuit, reference temperature and irradiance in kW/m^2, respectively.

2.3 MPPT algorithm

The perturbation and observation (P&O) algorithm is applied to obtain the maximum power from the PV array. The most widely employed algorithms for MPPT is P&O approach. Fig. 3 shows the flowchart of the mechanism. According to the algorithm, with perturbing the voltage in one direction if the power increases, then the algorithm keeps on perturbing in the same direction. Otherwise, it perturbs in the opposite direction. When the algorithm reaches the MPP, it keeps on fluctuating around the MPP.

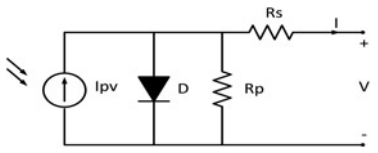

Fig. 2 *Equivalent circuit of PV array single diode model*

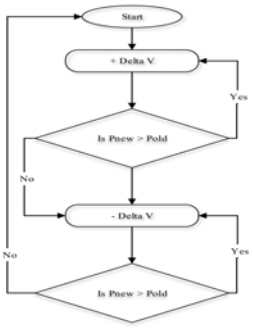

Fig. 3 *Basic algorithm of P&O MPPT*

2.4 Operating principle of three-phase PV

With considering balanced three-phase power grid voltage, following relations can be obtained:

$$\left\{\begin{array}{l} e_a = E\cos\omega t \\ e_b = E\cos(\omega t - 2\pi/3) \\ e_c = E\cos(\omega t + 2\pi/3) \end{array}\right\} \tag{4}$$

In above relations, E is defined as the peak value of voltage and ω is defined as the angular frequency of power grid. The fundamental relation of inverter can be expressed by Fig. 4

$$\begin{pmatrix} \frac{\mathrm{d}i_a}{\mathrm{d}t} \\ \frac{\mathrm{d}i_b}{\mathrm{d}t} \\ \frac{\mathrm{d}i_c}{\mathrm{d}t} \end{pmatrix} = \begin{pmatrix} -\frac{R}{L} & 0 & 0 \\ 0 & -\frac{R}{L} & 0 \\ 0 & 0 & -\frac{R}{L} \end{pmatrix}\begin{pmatrix} i_a \\ i_b \\ i_c \end{pmatrix} + \frac{1}{L}\begin{pmatrix} u_a & -e_a \\ u_b & -e_b \\ u_c & -e_c \end{pmatrix} \tag{5}$$

Coordinate transformation from three-phase stationary '*abc*' reference frame to two-phase synchronous rotating '*dq*' reference frame is given by (6)

$$\begin{pmatrix} \frac{\mathrm{d}i_d}{\mathrm{d}t} \\ \frac{\mathrm{d}i_q}{\mathrm{d}t} \end{pmatrix} = \frac{1}{L}\begin{pmatrix} -R & \omega\mathrm{L} \\ -\omega\mathrm{L} & -R \end{pmatrix}\begin{pmatrix} i_d \\ i_q \end{pmatrix} - \frac{1}{L}\begin{pmatrix} e_d \\ e_q \end{pmatrix} + \frac{1}{L}\begin{pmatrix} u_d \\ u_q \end{pmatrix} \tag{6}$$

In relation (6) i_d, i_q, u_d and u_q are the d-axis and q-axis components of three-phase grid-connected inverter output current, and output voltage, respectively. Here, e_d and e_q are the d-axis and q-axis components of three-phase grid voltage, respectively.

Relation (6) can be rewritten as follows:

$$\left\{\begin{array}{l} u_d = L\frac{\mathrm{d}i_a}{\mathrm{d}t} + Ri_d - \omega Li_q + e_d \\ u_q = L\frac{\mathrm{d}i_q}{\mathrm{d}t} + Ri_q + \omega Li_d + e_q \end{array}\right\} \tag{7}$$

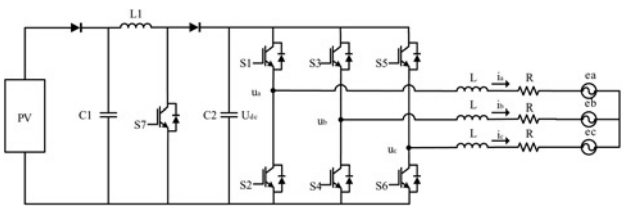

Fig. 4 *Schematic diagram of two-stage three-phase grid-connected inverter*

CIRED, Open Access Proc. J., 2017, Vol. 2017, Iss. 1, pp. 559–563

2.5 Analytical SRF method

Implementation of SRF with digital signal processor (DSP) algorithm because of its requirement of a phase-locked loop and a table to calculate cos ωt and sin ωt is very difficult. Low-pass filter (LPF) can eliminate all current harmonics, except DC value. Owing to the fact that harmonic frequencies are higher than DC frequency, thus, LPFs have higher performance. The LPF in traditional methods of SRF cannot eliminate the current second- and third-order harmonics in an unbalanced system. A new method based on mathematical analysis is proposed in [7].

Assuming balanced grid voltage, three-phase unbalanced non-linear load currents can be expressed as

$$\begin{aligned} i_{as} &= i_{as1} + i_{ash} \\ &= \sqrt{2} I_{a1} \sin(\omega t - \beta_{a1}) + \sqrt{2} \sum_{h \neq 1} I_{ah} \sin(h\omega t - \beta_{ah}) \end{aligned} \tag{8}$$

$$\begin{aligned} i_{bs} &= i_{bs1} + i_{bsh} = \sqrt{2} I_{b1} \sin\left(\omega t - \beta_{b1} - \frac{2\pi}{3}\right) \\ &\quad + \sqrt{2} \sum_{h \neq 1} I_{bh} \sin\left(h\omega t - \beta_{bh} - \frac{2\pi}{3}\right) \end{aligned} \tag{9}$$

$$\begin{aligned} i_{cs} &= i_{cs1} + i_{csh} = \sqrt{2} I_{c1} \sin\left(\omega t - \beta_{c1} + \frac{2\pi}{3}\right) \\ &\quad + \sqrt{2} \sum_{h \neq 1} I_{ch} \sin\left(h\omega t - \beta_{ch} + \frac{2\pi}{3}\right) \end{aligned} \tag{10}$$

where i_{js1} ($j = a, b, c$) is a fundamental component, J_{jsh} ($j = a, b, c$) is a harmonic component and β_{jh}, β_{j1} are the displacement power factor angles for the fundamental and harmonic components, respectively. Using the dq transformation for the above three-phase currents, we have

$$i^e_{dqns} = \begin{bmatrix} i^e_{ds} & i^e_{qs} & i^e_{ns} \end{bmatrix}^{\mathrm{T}} = T(\theta) i_{abcs} \tag{11}$$

where $i_{abcs} = \begin{bmatrix} i_{as} & i_{bs} & i_{cs} \end{bmatrix}^{\mathrm{T}}$ are D-axis and Q-axis components on the SRF which separated as

$$i^e_{dqs} = \begin{bmatrix} i^e_{ds} \\ i^e_{qs} \end{bmatrix} = \frac{\sqrt{2}}{3} \begin{bmatrix} i^e_{dsa} + i^e_{dsb} + i^e_{dsc} \\ i^e_{qsa} + i^e_{qsb} + i^e_{qsc} \end{bmatrix} \tag{12}$$

Each component of relation (12) can be defined as below:

$$i^e_{dsa} = \sqrt{2} i_{as} \sin\theta \tag{13}$$

$$i^e_{qsa} = \sqrt{2} i_{as} \cos\theta \tag{14}$$

$$i^e_{dsb} = \sqrt{2} i_{bs} \sin\left(\theta - \frac{2\pi}{3}\right) \tag{15}$$

$$i^e_{qsb} = \sqrt{2} i_{bs} \cos\left(\theta - \frac{2\pi}{3}\right) \tag{16}$$

$$i^e_{dsc} = \sqrt{2} i_{cs} \sin\left(\theta + \frac{2\pi}{3}\right) \tag{17}$$

$$i^e_{qsc} = \sqrt{2} i_{cs} \cos\left(\theta + \frac{2\pi}{3}\right) \tag{18}$$

Each of these quantities is divided into two frequencies, the main and harmonic, as follows:

$$i^e_{dsj} = i^{e1}_{dsj} + i^{eh}_{dsj} \tag{19}$$

$$i^e_{qsj} = i^{e1}_{qsj} + i^{eh}_{qsj} \tag{20}$$

where i^{e1}_{dqsj} is the fundamental component of i^{eh}_{dqsj} is the harmonic component of i_{jsh}.The detail relations for phase-a are reached from above are

$$\begin{aligned} i^e_{dsa} &= I_{a1}\{\cos\beta_{a1} - \cos(2\omega t - \beta_{a1})\} \\ &\quad + \sum_{h \neq 1} I_{ah}\{\cos\{(h-1)\omega t - \beta_{ah}\} - \cos\{(h+1)\omega t - \beta_{ah}\}\} \end{aligned} \tag{21}$$

$$\begin{aligned} i^e_{qsa} &= I_{a1}\{\sin(2\omega t - \beta_{a1}) - \sin\beta_{a1}\} \\ &\quad + \sum_{h \neq 1} I_{ah}\{\sin\{(h+1)\omega t - \beta_{ah}\} - \sin\{(h-1)\omega t - \beta_{ah}\}\} \end{aligned} \tag{22}$$

where i_{j1} is the fundamental current root-mean-square (RMS) value and i^e_{dqsj} is d-axis and q-axis components on the SRF.

It can be concluded from (21) and (22) that

$$\begin{aligned} i^{e1}_{dsa} &= I_{a1}\cos\beta_{a1} - I_{a1}\cos(2\omega t - \beta_{a1}) \\ &= I^{dc}_{dsa} - I_{a1}\{\cos(2\omega t)\cos\beta_{a1} + \sin(2\omega t)\sin\beta_{a1}\} \end{aligned} \tag{23}$$

$$\begin{aligned} i^{e1}_{qsa} &= I_{a1}\sin\beta_{a1} - I_{a1}\{\sin(2\omega t - \beta_{a1})\} \\ &= I^{dc}_{qsa} + \{\sin(2\omega t)\cos\beta_{a1} + \cos(2\omega t)\sin\beta_{a1}\} \end{aligned} \tag{24}$$

where I^{dc}_{dsa} and I^{dc}_{qsa} denote DC components. A simple first-order LPF with a cut-off frequency, ω_c can acquire the average value of DC component, i^{e1}_{dqsj}.

However, lower cut-off frequencies offer better filtering, the response time for load variations is slow. Since the DC quantity is available from an LPF, latter relations can be expressed from (23) and (24)

$$I^{dc}_{dsa} = I_{a1}\cos\beta_{a1} \tag{25}$$

$$I^{dc}_{qsa} = I_{a1}\sin\beta_{a1} \tag{26}$$

where I^{dc}_{dsa} denotes the d-axis component of phase current magnitude and I^{dc}_{qsj} denotes the q-axis component of displacement power factor angle I^{dc}_{qsj}. From the d-axis and q-axis components, the displacement power factor angle and fundamental current RMS value are obtained as

$$\beta^I_j = \tan^{-1}\left(-\frac{I^{dc}_{qsj}}{I^{dc}_{dsj}}\right) \tag{27}$$

$$I_{jI} = \frac{I^{dc}_{dsj}}{\cos\beta_{jI}} = -\frac{I^{dc}_{qsj}}{\sin\beta_{jI}} = \sqrt{I^{dc2}_{dsj} + I^{dc2}_{qsj}} \tag{28}$$

The SRF dq transformation can provide neutral expression i^e_{ns}

$$\begin{aligned} i^e_{ns} &= \frac{2}{3}\left\{I_{a1}\sin(\omega t - \beta_{a1}) + I_{b1}\sin\left(\omega t - \beta_{a1} - \frac{2\pi}{3}\right)\right. \\ &\quad \left. + I_{c1}\sin\left(\omega t - \beta_{c1} + \frac{2\pi}{3}\right)\right\} + \frac{2}{3}\sum_{h \neq 1}\left\{I_{ah}\sin(h\omega t - \beta_{ah})\right. \\ &\quad \left. + I_{bh}\sin\left(h\omega t - \beta_{hh} - \frac{2\pi}{3}\right) + I_{ch}\sin\left(h\omega t - \beta_{ch} + \frac{2\pi}{3}\right)\right\} \end{aligned} \tag{29}$$

where $i_{ns}^{e} = i_{ns}^{e1} + i_{ns}^{eh}$. Here, i_{ns}^{e1} can be computed by transforming unbalanced fundamental currents

$$i_{ns}^{e1} = \frac{2}{3}\left\{\begin{array}{l} I_{dsa}^{dc}\sin\omega t + I_{qsa}^{dc}\cos\omega t + I_{dsb}^{dc}\sin\left(\omega t - \frac{2\pi}{3}\right) \\ +I_{qsb}^{dc}\cos\left(\omega t - \frac{2\pi}{3}\right) + I_{dsc}^{dc}\sin\left(\omega t + \frac{2\pi}{3}\right) \\ +I_{qsc}^{dc}\cos\left(\omega t + \frac{2\pi}{3}\right) \end{array}\right\} \quad (30)$$

where i_{ns}^{e1} denotes the fundamental current for unbalanced condition. Fig. 5 shows obtained three-phase stationary frame currents, i.e. i_{ns}^{e1}, i_{qs}^{e1} and $i_{ds}^{e1}i_{ns}^{e1}$, i_{qs}^{e1} and i_{ds}^{e1}, the fundamental and harmonic currents.

Given to the complexity of the fundamental and harmonic calculation technique for practical implementation, thus, the per-phase approach is introduced for simplifying the implementation. We can reach to the following relations:

$$i_{ns}^{e1} = \frac{\sqrt{2}}{3}\left(i_{as1} + i_{bs1} + i_{cs1}\right) = \frac{\sqrt{2}}{3}i_{ns} \quad (31)$$

Since the phases b and c currents are null, single-phase fundamental current i_{as1}, is expressed by

$$i_{as1} = \frac{3}{\sqrt{2}}i_{ns}^{e1} \quad (32)$$

Simplified block diagram of single-phase system is shown in Fig. 6. Therefore, per-phase fundamental current is obtained without the requirement of other phases currents. The per-phase method needed two LPFs in each phase. Harmonic reference currents are calculated from

$$i_{jsh} = i_{js1} - i_{js} \quad (33)$$

This calculation approach can be employed either in a balanced or unbalanced conditions and has a good performance in the presence of current harmonic distortion.

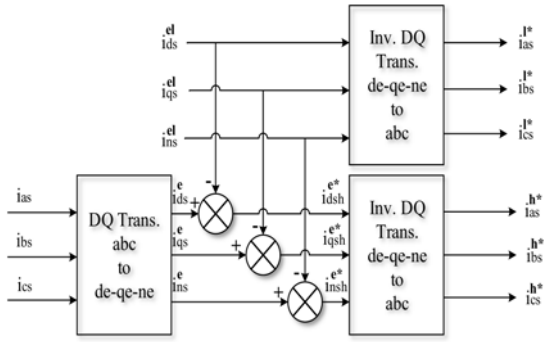

Fig. 5 *Fundamental and harmonic calculations*

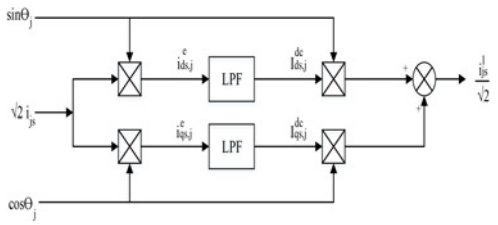

Fig. 6 *Fundamental current calculation based on per-phase approach*

2.6 Synchronous current detection

A scheme to keep current source sinusoidal has been introduced in [8]. Assuming that the source line currents are the same after compensation, results in

$$I_{ma} = I_{mb} = I_{mc} = I_m \quad (34)$$

$$I_{mk} = \frac{2P_k}{V_{mk}} \quad k = a,\ b,\ c \quad (35)$$

where p_k, $k = a$, b and c are average active powers that drawn by loads and V_{mk}, $k = a$, b and c are the peak values of phase voltage.

Considering above equations following relations are obtained:

$$\frac{P_k}{V_{mk}} = \frac{p_a + p_b + p_c}{V_{ma} + V_{mb} + V_{mc}}, \quad k = a,\ b,\ c \quad (36)$$

$$i_{sk} = I_{mk}\left(\frac{V_k}{V_{mk}}\right) = 2\left(\frac{p_k}{V_{mk}^2}\right)V_k, \quad k = a,\ b,\ c \quad (37)$$

where V_{sk} and i_{sk} are voltage and current of system, respectively. Therefore, the compensated current by active source filter is

$$i_{fk}^{*} = i_{lk} - \frac{2p_{T^{V_k}}}{V_{T^{V_{mk}}}}, \quad k = a,\ b,\ c \quad (38)$$

where $V_T = V_{ma} + V_{mb} + V_{mc}$, $p_T = p_a + p_b + p_c$.

3 Simulation results

Modified hysteresis PWM is useful in the creation of proper inverter pulses and is helpful for the production of compensated current by the inverter. Hence, the modelling based on this method is chosen. A typical network includes a non-linear load in order to confirm the performance of the algorithm is simulated. Simulations of a

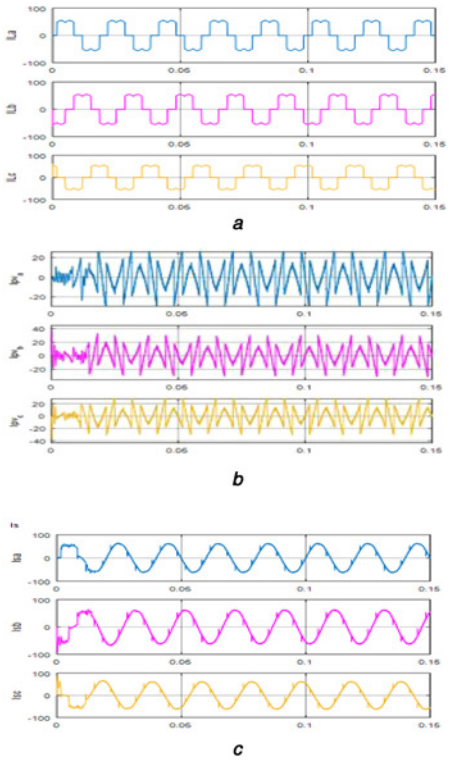

Fig. 7 *Simulations of a three-phase grid-connected system*

(a) Load current, ***(b)*** Current injection of PV system, ***(c)*** Network current

CIRED, Open Access Proc. J., 2017, Vol. 2017, Iss. 1, pp. 559–563

Table 1 Simulated system parameters

network's voltage	400 V
network's frequency	50 Hz
coupling's inductance	1.2 mH
source's resistance	1 mΩ
DC link's voltage	850 V
DC link's capacitance	0.00001 F
proportional gain (K_p)	10
integral gain (K_i)	100

three-phase grid-connected system with a non-linear load in order to verify the accuracy of the suggested algorithm is implemented by numeric simulation using the MATLAB/Simulink tools as shown in Fig. 7*a*. Moreover, in order to carry out the simulation tests close to the practical system, all parts of the system are discretised including the algorithms, data acquisition signals and controllers. Table 1 illustrates the simulated system parameters. The currents quantities of the PV–AF filter system is shown in Fig. 7. In this operation mode, the filter compensated the load reactive power and eliminated the load harmonic currents.

To confirm the performance of the suggested PV–AF system, it is tested in the presence of loads that drain currents with high total harmonic distortion (THD) from the grid. The tests are carried out when the PV–AF system is operating only as a shunt APF. The results are shown in Fig 8. A full-bridge diode rectifier followed by *R–C* load consists the non-linear load selected for the tests. In this case, the THD of the load current is around 30.30% which is shown in Fig. 8*a*. The PV–AF system has reduced the THD of the grid current by 5.49%, in another word a great decreasing of the grid current harmonics is cancelled out, which is shown in Fig. 8*b*.

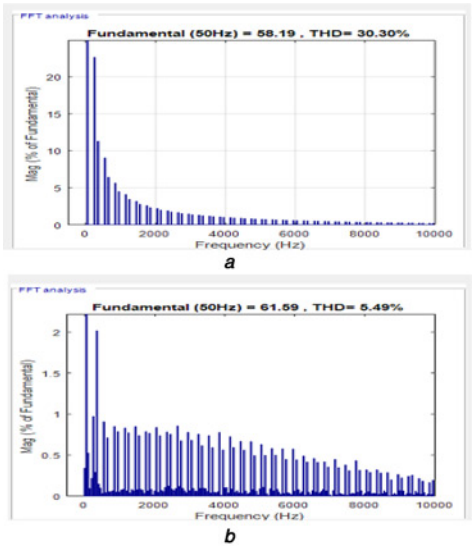

Fig. 8 *Results*

(a) Network current's THD without PV system, ***(b)*** Network current's THD with PV system

4 Conclusion

In this paper, implementation of a three-phase grid-tied PV–AF system is proposed. It is applied to a three-phase AC power system for active power injection, harmonic current elimination and reactive power compensation. The PV system is connected to the power grid with a DC/DC step-up converter and DC/AC full-bridge inverter. The equivalent model including nine panels connected in series constitutes the implemented PV system. The current reference integrated with the full-bridge inverter obtained by the analytical SRF algorithm adapted for three-phase systems applications. The performances of the system active power injection and/or reactive power compensation, and current harmonics elimination confirmed by the results. The effectiveness of the PV–AF system is verified by assuming two different loads draining currents from the grid with different THDs. The PV–AF system is capable of eliminating a high amount of harmonic currents and injecting active power into the power grid with low-THD current.

5 References

1 Bizzarri, F., Bongiorno, M., Brambilla, A., *et al.*: 'Model of photovoltaic power plants for performance analysis and production forecast', *IEEE Trans. Sustain. Energy*, 2013, **4**(2), pp. 278–285
2 Liu, Y., Xin, H., Wang, Z., *et al.*: 'Control of virtual power plant in microgrids: a coordinated approach based on photovoltaic systems and controllable loads'. Generation, Transmission & Distribution, IET 9, 2015, no. 10, pp. 921–928
3 Moradi-Shahrbabak, Z., Tabesh, A., Yousefi, G.R.: 'Economical design of utility-scale photovoltaic power plants with optimum availability'. IEEE Transactions on 61 Industrial Electronics, 2014, no. 7, pp. 3399–3406
4 Castilla, M., Miret, J., Camacho, A., *et al.*: 'Reduction of current harmonic distortion in three-phase grid-connected photovoltaic inverters via resonant current control'. IEEE Transactions on 60 Industrial Electronics, 2013, no. 4, pp. 1464–1472
5 Singh, B., Al-Haddad, K., Chandra, A.: 'A review of active filters for power quality improvement'. IEEE Transactions on 46 Industrial Electronics, 1999, no. 5, pp. 960–971
6 Hamid, M.I., Jusoh, A., Anwari, M.: 'Photovoltaic plant with reduced output current harmonics using generation-side active power conditioner'. IET 8 Renewable Power Generation, 2014, no. 7, pp. 817–826
7 Kim, S.: 'Harmonic reference current generation for unbalanced nonlinear loads', Power Electronics Specialist Conf., 2003. PESC'03 2003 IEEE 34th Annual, 2003, vol. 2, pp. 773–778
8 Chen, C.L., Lin, C.E., Huang, C.L.: 'An active filter for unbalanced three-phase system using synchronous detection method'. Power Electronics Specialists Conf. PESC'94 Record 25th Annual IEEE, 1994, pp. 1451–1455